

1 **Incursions of southern-sourced water into the deep North Atlantic**
2 **during Late Pliocene glacial intensification**

3

4 David C. Lang, Ian Bailey*, Paul A. Wilson, Thomas B. Chalk, Gavin L. Foster,
5 Marcus Gutjahr

6

7 **Affiliations**

8 David C. Lang

9 National Oceanography Centre Southampton, University of Southampton, Waterfront
10 Campus, Southampton SO14 3ZH, UK.

11

12 Ian Bailey

13 National Oceanography Centre Southampton, University of Southampton, Waterfront
14 Campus, Southampton SO14 3ZH, UK.

15 Now at: Camborne School of Mines and Environment and Sustainability Institute,
16 College of Engineering, Mathematics & Physical Sciences, University of Exeter,
17 Penryn Campus, Treliiever Road, Penryn, Cornwall TR10 9FE, UK.

18 ***Corresponding author**

19 Correspondence to: Ian Bailey, I.Bailey@exeter.ac.uk.

20

21 Paul A. Wilson

22 National Oceanography Centre Southampton, University of Southampton, Waterfront
23 Campus, Southampton SO14 3ZH, UK.

24

25 Thomas B. Chalk

26 National Oceanography Centre Southampton, University of Southampton, Waterfront
27 Campus, Southampton SO14 3ZH, UK.

28 Now at: Department of Physical Oceanography, Woods Hole Oceanographic
29 Institution, Woods Hole, MA 02543, USA.

30

31 Gavin L. Foster

32 National Oceanography Centre Southampton, University of Southampton, Waterfront
33 Campus, Southampton SO14 3ZH, UK.

34

35 Marcus Gutjahr

36 National Oceanography Centre Southampton, University of Southampton, Waterfront
37 Campus, Southampton SO14 3ZH, UK.

38 Now at: GEOMAR Helmholtz Centre for Ocean Research Kiel, Wischhofstraße 1–3,
39 24148 Kiel, Germany.

40

41 **The circulation and internal structure of the oceans exert a strong influence on**
42 **Earth's climate because they control latitudinal heat transport and the**
43 **segregation of carbon between the atmosphere and the abyss¹. Circulation**
44 **change, particularly in the Atlantic Ocean, is widely suggested²⁻⁵ to have been**
45 **instrumental in the intensification of northern hemisphere glaciation when large**
46 **ice-sheets first developed on North America and Eurasia during the Late**
47 **Pliocene, ~2.7 million years ago⁶. Yet the mechanistic link and cause/effect**
48 **relationship between ocean circulation and glaciation are debated. Here we**
49 **present new records of North Atlantic Ocean structure using the carbon and**
50 **neodymium isotopic composition of deep waters for both the Last Glacial to**
51 **Holocene (35-5 thousand years ago) and the Late Pliocene to earliest Pleistocene**
52 **(3.3 to 2.4 million years ago). Our data show no secular change. Instead we**
53 **document major southern-sourced water incursions into the deep North Atlantic**
54 **during prominent glacials from 2.7 million years ago. Our results suggest that**
55 **Atlantic circulation acts as a positive feedback rather than as an underlying**
56 **cause of Late Pliocene northern hemisphere glaciation. We propose that, once**
57 **surface Southern Ocean stratification⁷ and/or extensive sea-ice cover⁵ was**
58 **established, cold-stage expansions of southern-sourced water such as those**
59 **documented here enhanced carbon dioxide storage in the deep ocean, helping to**
60 **increase the amplitude of glacial cycles.**

61

62 During the Last Glacial Maximum (LGM, ~26-19.5 thousand years ago, ka) nutrient
63 (carbon)-poor North Atlantic Deep Water (NADW), or northern component waters
64 (NCW) were replaced at depth in the western North Atlantic by nutrient (carbon)-
65 enriched southern-component waters (SCW)⁸, although the precise relationship
66 between this orbitally paced change in ocean structure and Atlantic Meridional
67 Overturning Circulation (AMOC) is uncertain^{8,9}. Ocean circulation change is also

68 suggested²⁻⁵ to have played an important role in driving Earth's last major transition
69 in secular climate state, the intensification of northern hemisphere glaciation (NHG)
70 (~3.6-2.4 million years ago, Ma¹⁰). Here we test this hypothesis by constructing new
71 records of water mass mixing in the deep North Atlantic Ocean using two proxies:
72 carbon isotopes ($\delta^{13}\text{C}$) in benthic foraminiferal calcite and the neodymium (Nd)
73 isotope composition (ϵ_{Nd}) of fish debris. Our records come from the benchmark site
74 for monitoring the water mass structure of the deep Plio-Pleistocene North Atlantic,
75 Deep Sea Drilling Project (DSDP) Site 607¹¹⁻¹⁵ and its reoccupation¹⁶, Integrated
76 Ocean Drilling Program (IODP) Site U1313 (~41°N and 3427 m depth) situated in the
77 core of modern NADW.

78
79 The first reconstructions of water mass mixing during the intensification of NHG used
80 $\delta^{13}\text{C}$ from Site 607^{11,12} and concluded that prominent glaciations from ~2.5 Ma were
81 associated with suppression of NCW in the deep North Atlantic, but that NCW
82 production was always greater during NHG intensification than during the Late
83 Pleistocene glaciations. Subsequent $\delta^{13}\text{C}$ -based investigations^{3,13-15} concluded,
84 however, that NHG intensification was not associated with any major reorganization
85 of North Atlantic circulation, but was instead characterized by the persistence of
86 NCW in the deep Atlantic and of SCW in the deep South Atlantic throughout this
87 time. That interpretation is at odds with suggestions that either a major spin-up² or a
88 slow down⁵ in AMOC played a key role in driving NHG intensification.

89
90 Our ability to reconstruct water mass mixing using benthic $\delta^{13}\text{C}$ is complicated by the
91 potential for biological modification of this signal¹⁴ and published estimates of the
92 relative abundance of NCW (versus SCW) bathing the deep North Atlantic (%NCW)
93 during NHG intensification are compromised by use of low resolution $\delta^{13}\text{C}$ data and
94 unsuitable end-member records (see S1 in supplementary information). To address
95 these issues we present two new independent estimates of %NCW over the past 3.3
96 Myr based on: (i) published benthic $\delta^{13}\text{C}$ from Site 607 (for <2.4 Ma^{11,12}) and Site
97 U1313 for 3.3 to 2.4 Ma¹⁶ (which has twice the temporal resolution of the record from
98 Site 607 for the NHG intensification interval; Fig. 1); and (ii) new records of the ϵ_{Nd}
99 of fish debris at Site U1313 for both the Last Glacial to Holocene (35–5 ka) and the
100 Late Pliocene to earliest Pleistocene (1 sample every 6 kyr, 3.3–2.4 Ma; Fig. 2). Fish
101 debris fluorapatite acquires a bottom water ϵ_{Nd} signature during early stage diagenesis

102 that is retained on geological timescales under widely divergent preservation
103 conditions¹⁷. Ocean ϵ_{Nd} acts as a quasi-conservative water-mass tracer because the
104 ocean residence time of Nd (400–700 years¹⁷) is short relative to the whole ocean
105 mixing time (~1500 years) allowing water masses originating in different ocean
106 basins to bear distinct ϵ_{Nd} signatures (reflecting spatial heterogeneity in the age and
107 lithology of material added to surface oceans and ocean continental-margin sediment
108 boundary exchange processes¹⁷). The unradiogenic present day composition of NCW
109 (modern NADW, $\epsilon_{Nd} \sim -13.5$, Ref. 17) reflects the ancient continental crust
110 surrounding sites of North Atlantic Deep-Water formation, while Pacific Deep Water
111 (typically $\epsilon_{Nd} \sim -3$ to -6 , Ref. 17) and SCW end-members (modern Antarctic Bottom
112 Water and Antarctic Intermediate Water, $\epsilon_{Nd} \sim -7$ to -9 , Ref. 17) bear more radiogenic
113 values. Bottom water ϵ_{Nd} can be modified through ‘boundary exchange’ with ocean
114 sediments¹⁸ but, unlike $\delta^{13}C$, ϵ_{Nd} is independent of the carbon cycle¹⁷, which
115 underwent major change during NHG intensification¹⁹. Thus, application of two
116 proxies with different controls provides a way to improve our understanding of NCW
117 history during this time.

118

119 In Figure 2 we present new ϵ_{Nd} records from Site U1313 for the Last Glacial through
120 mid-Holocene and for NHG intensification from the deep North Atlantic and compare
121 them to other ϵ_{Nd} data sets and the $\delta^{13}C$ records from Figure 1. Our ϵ_{Nd} record for the
122 Last Glacial shows the same isotopic composition and closely follows published
123 records from the deep western North Atlantic (ϵ_{Nd} LGM > Holocene by ~ 3.5 ϵ -
124 units)^{8,18,20}, demonstrating a clear incursion of radiogenic SCW into the deep North
125 Atlantic during the LGM. Based on the age model of Ref. 21, and our new records of
126 coarse lithic deposition at Site U1313 (Fig. 2c), changes in bottom water ϵ_{Nd} suggest
127 that the return of NADW during the last deglacial may occur at our study site during
128 Heinrich (H)-event 1, ~ 18 ka, ~ 3 kyrs earlier than at deeper (>4500 m) and more
129 southerly sites (Fig. 2a). This finding may be attributable to the more proximal
130 location of Site U1313 to the Labrador Sea compared to Bermuda Rise, or
131 alternatively, bottom water ϵ_{Nd} at Site U1313 may be influenced by unradiogenic-
132 labeling of deepwaters by massive episodes of ice-rafted detrital-carbonate deposition
133 upstream of our study site during H1²² (see supplementary information, S4).
134 Regardless, our records show that, outside of H-events, ϵ_{Nd} data from Site U1313

135 track the pattern of Last Glacial SCW incursion into the deep North Atlantic well
136 documented by other proxy records⁹.
137
138 Our new Nd isotope record for NHG intensification exhibits a range of ϵ_{Nd} values (-
139 9.6 to -13.1 = 3.5 ϵ -units) similar to the amplitude of change (-11 to -14.5 = 3.5 ϵ -
140 units) documented for the Last Glacial transition (Fig. 2e,f). During the mid-
141 Piacenzian Warm Period (~3.3-3 Ma), Site U1313 is characterized by unradiogenic
142 values (Fig. 2b) similar to those observed for NCW as observed in contemporaneous
143 Fe-Mn crust records precipitated in the shallow North Atlantic (1.9-2.65 km). In
144 contrast in a number of cold stages during NHG intensification (MIS M2, G16, G6,
145 100 and 96) and one interglacial (MIS K1), our Nd record shows prominent
146 radiogenic excursions that must reflect either significant changes in NCW ϵ_{Nd} or times
147 of increased influence of SCW on bottom waters at Site U1313 (see S2-4 in
148 supplementary information). Analogy to our Last Glacial record strongly supports the
149 latter explanation, thus providing the first evidence for a number of LGM-magnitude
150 incursions of SCW into the deep North Atlantic during NHG intensification. To
151 explore these events further we employ simple binary mixing equations (see methods,
152 and supplementary information, S1-2) to both the ϵ_{Nd} and $\delta^{13}C$ records from Site
153 607/U1313.
154
155 Both of our %NCW records (Figs. 1b, 2g-h) show significant excursions towards
156 SCW values during NHG intensification (with reductions in %NCW down to 60%)
157 consistent with published reconstructions^{11,12}, albeit not as clearly expressed in the
158 lower resolution Site 607 $\delta^{13}C$ record (Fig. S4e). Comparison of our %NCW $_{\delta^{13}C}$ and
159 %NCW $_{\epsilon_{Nd}}$ records shows that the significant radiogenic excursions in ϵ_{Nd} at Site
160 U1313 during MIS M2, 3.3 Ma, and MIS K1, ~3.07 Ma, (Fig. 2b,h) are not supported
161 by our $\delta^{13}C$ -based record (Fig. 2h,j). Similarly, a number of cold stages between ~3
162 and 2.75 Ma show %NCW $_{\delta^{13}C}$ reductions that are not evident in %NCW $_{\epsilon_{Nd}}$. Our
163 understanding of the history of %NCW prior to ~2.72 Ma will improve when our
164 knowledge of NCW and SCW end-member compositions is refined. Meanwhile, the
165 good correspondence between our two records from ~2.72 Ma onwards strongly
166 suggests that SCW incursions during MIS G6, 100 and 96 were comparable to the
167 LGM. This inference is supported by LGM-magnitude cooling of bottom water

168 temperatures at Site 607 during these three glacials, presumably reflecting the arrival
169 of cold SCW in the deep North Atlantic (Fig. 3a, b). We also note that these events
170 correlate with pronounced cooling of mid-latitude and/or Arctic surface temperatures
171 (Fig. 3a-c).

172

173 Our evidence for Southern Ocean incursions into the deep North Atlantic provides
174 fresh insight into the relationship between North Atlantic circulation and NHG
175 intensification (Fig 3). Numerical models of ocean circulation suggest that any
176 substantial secular slowdown in overturning of the NCW cell during NHG
177 intensification would be registered by shoaling of its lower boundary²³ and hence a
178 change in ϵ_{Nd} at Site U1313 on a corresponding timescale. Instead the most prominent
179 feature of our records is that they exhibit enhanced excursions during cold-stages
180 rather than any long-term secular change (Fig. 2). We also observe the development
181 of a lag in ϵ_{Nd} relative to changes in benthic $\delta^{18}O$ at Site U1313 from ~ 2.9 Ma
182 (typically of 4-9 kyr, Fig. S11), analogous to the Late Pleistocene (e.g., Ref. 8). These
183 observations suggest a response of Atlantic circulation to, rather than secular forcing
184 of glaciation.

185

186 Long-term expansion of the Antarctic Ice Sheet and coastal sea-ice between ~ 3.3 and
187 2.6 Ma^{4,5,24}, bi-polar surface water stratification from ~ 2.7 Ma⁷ and increased heat
188 transport from the northern hemisphere to the deep Pacific from this time⁴ during
189 warm but not cold stages (this study) helped to precondition the northern hemisphere
190 for significant continental glaciation by cooling the Arctic and by enhancing storage
191 of carbon dioxide in the abyss. We suggest that, once these preconditions were met
192 (Fig. 3g-h), incursions of SCW into the deep North Atlantic acted as a positive
193 feedback to amplify glacial cycles from ~ 2.72 Ma through increased sequestration of
194 carbon in the deep Atlantic¹, contributing to the observed^{4,5} tighter coupling of inter-
195 hemisphere climate on orbital timescales from this time (Fig. 3). One prediction of
196 this hypothesis is that further improvements to the proxy record of atmospheric CO_2
197 levels¹⁹ will reveal an amplified signal at the obliquity scale from ~ 2.7 Ma.

198

199 It is debated whether Southern Ocean water incursions into the deep Atlantic during
200 the Last Glacial Cycle were driven by southern polar ocean conditions, notably

201 deepwater densification through increased sea-ice formation (a proposed driver of
202 LGM NADW shoaling²⁵) or by reductions in NCW formation during the LGM
203 because of sensitivity to freshwater forcing⁸ in the North Atlantic and/or sea ice
204 expansion in the Nordic Seas. For NHG intensification, the close association between
205 major SCW incursions at Site U1313 and evidence for the onset of major ice-rafted
206 debris (IRD) deposition across both the Nordic Seas²⁶ and North Atlantic⁶ from ~2.72
207 Ma onwards (Fig. 3f) suggests that SCW incursions into the deep North Atlantic were
208 perhaps driven by northern forcing agents. On the other hand, step-wise expansion of
209 the Antarctic Ice Sheet ~3.3 Ma is thought⁵ to have triggered the initiation of quasi-
210 permanent Antarctic sea ice formation (Fig 3g,h). Hence, if as suggested by our ϵ_{Nd}
211 record, major incursions of SCW into the deep Atlantic date to MIS M2 (i.e., well
212 before the onset of major NHG^{6,27,28}; Fig. 3e) then a southern hemisphere forcing
213 mechanism is implied.

214

215 References

- 216 1. Sigman, D. M., Hain, M. P. & Haug, G. H. The polar ocean and glacial cycles
217 in atmospheric CO₂ concentration. *Nature* **466**, 47–55,
218 doi:10.1038/Nature09149 (2010).
- 219 2. Bartoli, G. et al. Final closure of Panama and the onset of northern hemisphere
220 glaciation. *Earth and Planetary Science Letters* **237**, 33–44 (2005).
- 221 3. Haug, G. H. & Tiedemann, R. Effect of the formation of the Isthmus of
222 Panama on Atlantic Ocean thermohaline circulation. *Nature* **393**, 673–676
223 (1998).
- 224 4. Woodard, S. C. et al. Antarctic role in Northern Hemisphere glaciation.
225 *Science* **346**, 847–851, doi:10.1126/science.1255586 (2014)
- 226 5. McKay, R. et al. Antarctic and Southern Ocean influences on Late Pliocene
227 global cooling. *PNAS* **109**, 6423–6428,
228 www.pnas.org/cgi/doi/10.1073/pnas.1112248109 (2012).
- 229 6. Bailey, I. et al. An alternative suggestion for the Pliocene onset of major
230 northern hemisphere glaciation based on the geochemical provenance of North
231 Atlantic Ocean ice-rafted debris. *Quaternary Science Reviews* **75**, 181–194,
232 doi:10.1016/J.Quascirev.2013.06.004 (2013).
- 233 7. Sigman, D. M., Jaccard, S. L. & Haug, G. H. Polar ocean stratification in a
234 cold climate. *Nature* **428**, 59–63, doi:10.1038/nature02357 (2004).
- 235 8. Böhm, E. et al. Strong and deep Atlantic meridional overturning circulation
236 during the last glacial cycle. *Nature* **517**, 73–76 (2015).
- 237 9. Lynch-Stieglitz, J. et al. Atlantic meridional overturning circulation during the
238 Last Glacial Maximum. *Science* **316**, 66–69, doi:10.1126/science.1137127
239 (2007).
- 240 10. Lisiecki, L. E. & Raymo, M. E. A. Pliocene-Pleistocene stack of 57 globally
241 distributed benthic $\delta^{18}O$ records. *Paleoceanography* **20**, PA1003. doi:10.1029/
242 2005PA001153 (2005).

- 243 11. Raymo M. E., Ruddiman, W. F., Shackleton, N. J. & Oppo, D. W. Evolution
244 of Atlantic- Pacific $\delta^{13}\text{C}$ gradients over the last 2.5 m.y. *Earth and Planetary*
245 *Science Letters* **97**, 353–368 (1990).
- 246 12. Raymo, M. E, Hodell, D. A. & Jansen, E. Response of deep ocean circulation
247 to initiation of Northern Hemisphere glaciation (3–2 Ma). *Paleoceanography*
248 **7**, 645–672, doi:10.1029/92PA01609 (1992).
- 249 13. Venz, K. A. & Hodell, D. A. New evidence for changes in Plio-Pleistocene
250 deep water circulation from Southern Ocean ODP Leg 177 Site 1090.
251 *Palaeogeography, Palaeoclimatology, Palaeoecology* **182**, 197–220 (2002).
- 252 14. Hodell, D. A. & Venz-Curtis, K. A. Late Neogene history of deepwater
253 ventilation in the Southern Ocean. *Geochemistry Geophysics Geosystems* **7**,
254 Q01003. doi:10.1029/2005gc001211 (2006).
- 255 15. Lisiecki, L. E. Atlantic overturning responses to obliquity and precession over
256 the last 3 Myr. *Paleoceanography* **29**, 71–86, doi:10.1002/2013pa002505
257 (2014).
- 258 16. Lang, D. C. et al. The transition on North America from the warm humid
259 Pliocene to the glaciated Quaternary traced by eolian dust deposition at a
260 benchmark North Atlantic Ocean drill site. *Quaternary Science Reviews* **93**,
261 125–141, doi:10.1016/j.quascirev.2014.04.005 (2014).
- 262 17. Frank, M. Radiogenic isotopes: Tracers of past ocean circulation and erosional
263 input. *Reviews of Geophysics* **40**, 1-1-1-38, doi:10.1029/2000rg000094 (2002).
- 264 18. Roberts, N. L., Piotrowski, A. M., McManus, J. F. & Keigwin, L. D.
265 Synchronous deglacial overturning and water mass source changes. *Science*
266 **327**, 75–78, doi:10.1126/science.1178068 (2010).
- 267 19. Martínez-Botí, M. A. et al. Plio-Pleistocene climate sensitivity evaluated using
268 high-resolution CO_2 records. *Nature* **518**, 49–54, doi:10.1038/nature14145
269 (2015).
- 270 20. Gutjahr, M. & Lippold, J. Early arrival of Southern Source Water in the deep
271 North Atlantic prior to Heinrich event 2. *Paleoceanography* **26**, PA2101. doi:
272 10.1029/2011pa002114 (2011).
- 273 21. Naafs, B. D. A., Hefter, J., Grutzner, J. & Stein, R. Warming of surface waters
274 in the mid-latitude North Atlantic during Heinrich events. *Paleoceanography*
275 **28**, 153-163, doi:10.1029/2012pa002354 (2013).
- 276 22. Roberts, N. L., & Piotrowski, A. M. Radiogenic Nd isotope labeling of the
277 northern NE Atlantic during MIS 2. *Earth and Planetary Science Letters* **423**,
278 125–133 (2015).
- 279 23. Kostov, Y., Armour, K. C. & Marshall, J. Impact of the Atlantic meridional
280 overturning circulation on ocean heat storage and transient climate change,
281 *Geophys. Res. Lett.* **41(6)**, 2108–2116 (2014).
- 282 24. Hillenbrand C. -D. & Cortese, G. Polar stratification: A critical view from the
283 Southern Ocean. *Palaeogeog. Palaeoclimat. Palaeoecol.* **242**, 240–252
284 (2006).
- 285 25. Ferrari, R. et al. Antarctic sea ice control on ocean circulation in present and
286 glacial climates. *PNAS* **111**, 8753–8758, doi:10.1073/pnas.1323922111
287 (2014).
- 288 26. Jansen, E., Fronval, T., Rack, F. & Channell, J. E. T. Pliocene-Pleistocene ice
289 rafting history and cyclicity in the Nordic Seas during the last 3.5 Myr.
290 *Paleoceanography* **15(6)**, 709–721 (2000).
- 291 27. Balco, G. & Rovey II, C.W. Absolute chronology for major Pleistocene
292 advances of the Laurentide Ice Sheet, *Geology* **38**, 795–798,

- 293 <http://dx.doi.org/10.1130/G30946.1> (2010).
- 294 28. Brigham-Grette, J. et al. Pliocene Warmth, Polar Amplification, and Stepped
295 Pleistocene Cooling Recorded in NE Arctic Russia. *Science* **340**, 1421–1426,
296 doi:10.1126/science.1233137 (2013).
- 297 29. Sosdian, S. & Rosenthal, Y. Deep-sea temperature and ice volume changes
298 across the Pliocene-Pleistocene climate transitions. *Science* **325**, 306–310,
299 doi:10.1126/science.1169938 (2009).
- 300 30. Mix, A. C. et al. Benthic foraminifer stable isotope record from Site 849 (0-5
301 Ma): local and global climate changes. *Proc. ODP Scientific Results* **138**, 371–
302 412 (1995).
- 303 31. Bolton, C. T. et al. Millennial-scale climate variability in the subpolar North
304 Atlantic Ocean during the late Pliocene. *Paleoceanography* **25**, PA4218.
305 doi:10.1029/2010PA001951 (2010).
- 306 32. Naafs, B. D. A. et al. Strengthening of North American dust sources during the
307 late Pliocene (2.7 Ma). *Earth and Planetary Science Letters* **317**, 8–19 (2012).
- 308

309

310 **Acknowledgments**

311 This research used samples provided by IODP (sponsored by the US National Science
312 Foundation and participating countries under management of Joint Oceanographic
313 Institutions, Inc). We thank the shipboard party of IODP Expedition 306. We are
314 grateful to W. Hale, A. Weulbers, A. Milton, M. Cooper, M. Spencer and A. Michalik
315 for laboratory assistance, D. Murphy for assistance with fish debris identification and
316 C. Ullmann for assistance with data plotting. We also thank M. Hain and M. Raymo
317 for helpful discussions. This research was supported by the Natural Environment
318 Research Council (NERC) through a PhD studentship to DCL, a NERC UK IODP
319 grant NE/F00141X/1 to PAW and IB, a Royal Society Wolfson Research Merit
320 Award to PAW and NERC grant NE/H006273/1 to GLF.

321

322 **Author contributions**

323 IB and PAW designed the study. DCL picked, prepared and analysed fish debris for
324 their Nd isotope compositions with guidance from MG. IB generated the Last Glacial-
325 Holocene IRD record. DCL made initial interpretations of the data. IB and PAW
326 wrote the main text with input from GLF and MG. TBC and GLF performed Monte
327 Carlo simulations and statistical analyses. All authors discussed the results.

328

329 **Competing financial interests**

330 The authors declare no competing financial interests.

331

332 **Figure captions**

333 Fig. 1: Mixing history of northern- versus southern-sourced waters in the deep North
334 Atlantic (~3400 m) for the past 3.3 Myr based on benthic foraminiferal carbon
335 isotopes: **(a)** benthic $\delta^{13}\text{C}$ records from the shallow North Atlantic (ODP Site 982¹⁴),
336 deep North Atlantic (composite of Chain 82-24-23PC²⁹, DSDP Site 607¹¹, and
337 U1313¹⁶) and deep Pacific (ODP Site 849³⁰) **(b)** %NCW estimated using records
338 shown in (a) (purple line best estimate, shading 95% confidence interval, see
339 methods); **(c)** benthic foraminiferal $\delta^{18}\text{O}$ data from Site U1313 (purple³¹) and global
340 benthic $\delta^{18}\text{O}$ stack¹⁰ (black).

341

342 Fig. 2: Mixing history of northern- versus southern-sourced waters in the deep North
343 Atlantic, for 3.3-2.4 Ma and the Last Glacial-Holocene (35-5 ka): **(a & b)** fish debris
344 ϵ_{Nd} from IODP Site U1313 (purple; this study) and, in (a), ϵ_{Nd} of uncleaned planktic
345 foraminifera (brown¹⁸) and bulk sediment leachate (green^{8,20}) from Bermuda Rise
346 (error bars = 2σ uncertainty); **(c & d)** U1313 IRD concentration (40-5 ka, this study;
347 NHG intensification^{16,31}); ϵ_{Nd} deviation from mean (35-5 ka) **(e)** and 3.3-2.4 Ma **(f)**; **(g**
348 **& h)** %NCW at U1313 using ϵ_{Nd} (top) from (a & b, this figure) and $\delta^{13}\text{C}$ (bottom)
349 from Fig. 1b; purple line best estimate, shading 95% confidence interval; **(i-l)** benthic
350 foraminiferal $\delta^{13}\text{C}$, $\delta^{18}\text{O}$ and ϵ_{Nd} from U1313¹⁶/82-24-23PC²⁹ and benthic $\delta^{18}\text{O}$
351 stack¹⁰. Sources of crust and Cape Basin ϵ_{Nd} records used to define NCW and SCW
352 ϵ_{Nd} given in Tab. S3. Pink(blue) zones in (a) and (b) reflect ϵ_{Nd} range of NCW(SCW)
353 end-members used to estimate %NCW shown in (g) & (h) (see methods). Red bar in
354 (a) = range of modern NADW ϵ_{Nd} ¹⁷.

355

356 Fig. 3: Incursions of southern-sourced water into the deep North Atlantic (~3400 m)
357 and relation to NHG intensification: **(a)** %NCW ϵ_{Nd} (purple line best estimate, shading
358 95% confidence interval); **(b)** alkenone-SST at Site U1313³² and Mg/Ca bottom water
359 temperature at Site 607²⁹; **(c)** Air temperature in Arctic NE Russia²⁸ **(d)** age range and
360 2σ uncertainty for oldest advance of Laurentide Ice Sheet into Missouri²⁷; **(e)** onset of
361 major NHG^{6,27,28}; **(f)** Ice-rafting to U1313^{16,31}, Site 611⁶ (52.5°N) and Site 907²⁶
362 (69°N); **(g)** Antarctic sea-ice evolution based on Site 1096 opal mass accumulation²⁴
363 and on AND-1B diatom species⁵; **(h)** glacial regime of marine Antarctic Ice Sheet in
364 Ross Embayment (AND-1B)⁵; **(i)** benthic $\delta^{18}\text{O}$ stack¹⁰.

365

366 **Methods**

367 To reconstruct the provenance of bottom waters bathing Site U1313 during NHG
368 intensification between 2.4 to 3.3 Ma (MIS MG1–95) we sampled on average every
369 30 cm (~6 kyr) from the shipboard primary splice (between 114.3 and 155.2 metres
370 composite depth, mcd) used to generate the published benthic $\delta^{18}\text{O}$ (Ref. 31) and $\delta^{13}\text{C}$
371 (Ref. 16) stratigraphies for our study site. Fish debris from sediments deposited at Site
372 U1313 during MIS 100, and from six samples on which detrital sediment ϵ_{Nd} values
373 were previously published¹⁶, were hand-picked from samples taken from the
374 secondary splice after placing the secondary splice onto the depth scale of the primary
375 splice via manual graphical correlation of shipboard-derived sediment lightness
376 records (L^* , here driven by variability in the sediment calcium carbonate content¹⁶,
377 Fig. S10). The age model for our record is based on tuning³¹ the Site U1313 benthic
378 $\delta^{18}\text{O}$ stratigraphy to the LR04 stack¹⁰. To generate a Last Glacial to Holocene ϵ_{Nd}
379 record for Site U1313 we sampled Holes C and D of this site every 7 to 14 cm from
380 0.2–1.76 mcd, ($n = 22$, see also Fig. S9) corresponding to an average sampling
381 resolution of ~1.3 kyr. The published age model²¹ that we use for our Last Glacial
382 record is based on correlation of H-layers in the Site U1313 stratigraphy (tracked by
383 XRD dolomite/calcite ratio data) to X-ray fluorescence-based Ca/Sr elemental data
384 that track the position of H-layers in the stratigraphy of northeast Atlantic Ocean
385 IODP Site U1308 (~50°N), which has a benthic $\delta^{18}\text{O}$ stratigraphy on LR04 ages³³.
386

387 We hand-picked fish debris (10 to 30 pieces of bones and teeth, depending on
388 availability) from the $>150\mu\text{m}$ fraction of disaggregated sediment. Samples were
389 cleaned with two steps of ultrasonication in methanol, followed by three rinses in
390 MilliQ H_2O . Organic material was removed by bathing each sample in an oxidising
391 solution (1% H_2O_2 – 0.1M NH_4OH) at 80°C for 30 minutes, while sonicating for 30
392 seconds every 10 minutes. A weak-acid (0.001M HNO_3) leach was applied to ensure
393 removal of any reabsorbed contaminants, before samples were dissolved in 0.1ml
394 1.75M HCl. Pure samples of Nd were separated following standard procedures^{34,35}.
395 Nd isotope ratios ($^{143}\text{Nd}/^{144}\text{Nd}$) were measured at the University of Southampton
396 using a multi-collector inductively coupled plasma mass spectrometer (MC-ICP-MS,
397 Thermo Scientific Neptune). Neodymium isotope compositions were obtained using

398 the method of Ref. 36 through adjustment to a $^{146}\text{Nd}/^{144}\text{Nd}$ ratio of 0.7219 and a
399 secondary normalization to $^{142}\text{Nd}/^{144}\text{Nd} = 1.141876$ (Ref. 36). Total procedural blanks
400 averaged 35 pg for fish debris. External reproducibility of the JNdi standard³⁷ was
401 ± 0.000006 (2 s.d.), corresponding to an external error of $\pm 0.13 \epsilon_{\text{Nd}}$ (2 s.d.). In all cases
402 we plot the external error, unless the internal error is larger than the external error
403 when we plot a combined error calculated as $\sqrt{(\text{external error}^2 + \text{internal error}^2)}$.
404 All Nd isotope ratios are reported in epsilon notation as:

405

$$406 \quad \epsilon_{\text{Nd}} = \left[\frac{{}^{143}\text{Nd}/{}^{144}\text{Nd}_{\text{sample}}}{{}^{143}\text{Nd}/{}^{144}\text{Nd}_{\text{CHUR}}} - 1 \right] \times 10^4$$

407

408 Radiogenic ingrowth of ^{143}Nd is corrected using a typical $^{147}\text{Sm}/^{144}\text{Nd}$ of 0.125 (Ref.
409 38). Corrections are within analytical uncertainty ($< 0.06 \epsilon_{\text{Nd}}$ for our NHG
410 intensification data, and negligible for Last Glacial–Holocene data), reflecting the
411 young age of our samples relative to the half-life of ^{147}Sm . We note that fish debris
412 $^{147}\text{Sm}/^{144}\text{Nd}$ ratios typically vary within a narrow range and that our results are
413 insensitive to the choice of this value.

414

415 A record of sand IRD abundance in sediments deposited at Site U1313 during NHG
416 intensification already exists^{16,31}. To assess the concentration of IRD in sediments for
417 the Last Glacial at our study site we performed new coarse lithic counts on the >150
418 μm size fraction between 0.2–2.43 mcd. To generate a statistically significant record
419 of sand IRD abundance in Site U1313 sediments (expressed as IRD per gram of dry
420 sediment) we identified the composition of at least 300 coarse lithics or where 300
421 grains were not present we counted all grains in the sample (where there were
422 typically only 1–30 total grains in Last Glacial sediments deposited outside of
423 Heinrich-events). In each case, our counts differentiated between volcanics, cream
424 coloured detrital limestone and other coarse lithics (predominantly quartz and
425 feldspar, plus minor numbers of other rock clasts).

426

427 To estimate the relative contribution of NCW bathing Site 607/U1313 over the past
428 3.3 Ma using benthic $\delta^{13}\text{C}$ datasets we used the following binary mixing equation:

429
$$\%NCW_{\delta^{13}C} = 100 * \left(\frac{\delta^{13}C_{(607/U1313)} - \delta^{13}C_{(SCW)}}{\delta^{13}C_{(NCW)} - \delta^{13}C_{(SCW)}} \right)$$

430 Where $\%NCW_{\delta^{13}C}$ is the relative contribution of NCW to waters bathing the deep
 431 North Atlantic Ocean ($\%SCW = 100 - \%NCW$), $\delta^{13}C_{(607/U1313)}$ is the carbon isotope
 432 composition of benthic foraminiferal calcite (predominantly determined from the
 433 epifaunal benthic foraminifera *Cibicidoides wuellerstorfi*) from the deep North
 434 Atlantic (Site 607/U1313), and $\delta^{13}C_{(NCW)}$ and $\delta^{13}C_{(SCW)}$ are the equivalent carbon
 435 isotope signatures of NCW (ODP Site 982, Ref. 14) and SCW (ODP Site 849, Ref.
 436 30), respectively (see supplementary information, S1, for further details).

437

438 To estimate the relative contribution of NCW and SCW to waters bathing IODP Site
 439 U1313 during NHG intensification and the last deglacial using Nd isotopes we used
 440 the following binary mixing equation constrained by our current understanding of
 441 end-member compositions and their Nd concentrations:

442
$$\%NCW_{\epsilon_{Nd}} = \frac{\frac{fnCs}{fsCn}}{1 + \frac{fnCs}{fsCn}} \times 100$$

443 Where $\%NCW_{\epsilon_{Nd}}$ is the relative contribution of NCW to waters bathing Site U1313
 444 ($\%SCW = 100 - \%NCW_{\epsilon_{Nd}}$) and $Cs =$ concentration of Nd in SCW, $Cn =$
 445 concentration of Nd in NCW. $fn =$ fraction of Nd coming from the north, such that:

446

447
$$fn = \frac{\epsilon_{NdU1313} - \epsilon_{NdSCW}}{\epsilon_{NdNCW} - \epsilon_{NdSCW}}$$

448

449 where $\epsilon_{NdU1313}$ is the Nd isotope value of fish debris from Site U1313, ϵ_{NdSCW} is the
 450 southern end member isotope composition and ϵ_{NdNCW} is the northern end member
 451 isotope composition; fs is then the fraction of Nd coming from the south which is
 452 equal to $1-fn$ in our binary mixing model (i.e. everything that is not from a northern
 453 source). To estimate the ϵ_{Nd} of NCW and SCW during NHG intensification we took
 454 the average value of all published Fe-Mn crust ϵ_{Nd} (and their 2s.d.) that span ~3.3-2.4
 455 Ma (Fig. 2b and Tab. S3). For our Last Glacial-Holocene record, following Ref. 39,
 456 NCW ϵ_{Nd} was defined as the average of our Holocene data (<14 ka; MIS 2/1
 457 boundary as defined by Ref. 10) from Site U1313 (and their 2s.d.) (Fig. 2a and Tab.
 458 S3). We define SCW ϵ_{Nd} for this time interval using a splice of Site RC11-83 &

459 TN057-21 ϵ_{Nd} ; Ref. 39; Tab. S3), which we resampled onto the ages of our Site
460 U1313 record (see S2 in supplementary information for further details). Confidence
461 intervals (95%) for %NCW are estimated using a Monte Carlo simulation (n=10,000)
462 performed in R⁴⁰, fully propagating analytical uncertainties, and uncertainties in the
463 ϵ_{Nd} of NCW and SCW and their Nd concentrations⁴¹ (see S2 in supplementary
464 information). To perform this exercise we make the following assumptions: (i) Nd
465 isotopes exhibit conservative behaviour, which is an acceptable approximation in
466 abyssal open ocean settings, (ii) mixing of NCW and SCW at Site U1313 is binary,
467 and (iii) that the modern day end-member [Nd] has remained constant over the past
468 ~3.3 Ma (see S2 in supplementary information).

469

470 To determine the lag-correlation of Site U1313 ϵ_{Nd} (this study), benthic $\delta^{13}\text{C}$ (Ref. 16)
471 and Site U1313 benthic $\delta^{18}\text{O}$ (Ref. 31) during NHG intensification (Fig. S11) we used
472 an auto-correlation function in R⁴⁰ every 50 kyr using a 200 kyr window. Before
473 analysing the data all records were resampled at a common 1 kyr resolution.

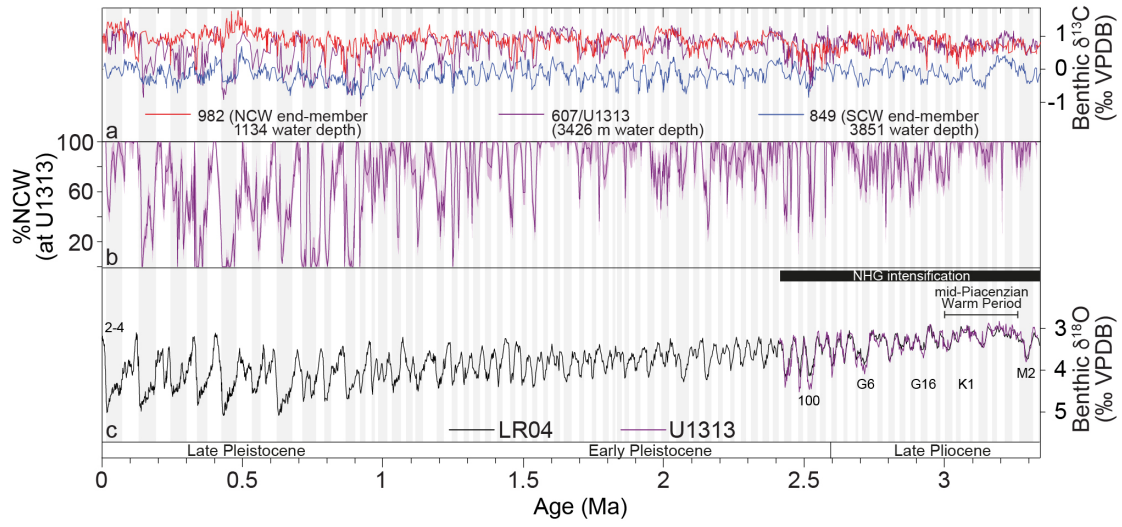
474

475 **Methods References**

- 476 33. Hodell, D. A., Channell, J. E. T., Curtis, J. H., Romero, O. E. & Röhl, U.
477 Onset of "Hudson Strait" Heinrich events in the eastern North Atlantic at the
478 end of the middle Pleistocene transition (~640 ka)? *Paleoceanography*
479 **PA4218**, doi:10.1029/2008PA001591 (2008).
- 480 34. Cohen, A. S., Onions, R. K., Siegenthaler, R. & Griffin, W. L. Chronology of
481 the Pressure-Temperature History Recorded by a Granulite Terrain.
482 *Contributions to Mineralogy and Petrology* **98**, 303–311,
483 doi:10.1007/Bf00375181 (1988).
- 484 35. Pin, C., Briot, D., Bassin, C. & Poitrasson, F. Concomitant separation of
485 strontium and samarium-neodymium for isotopic analysis in silicate samples,
486 based on specific extraction chromatography. *Anal. Chim. Acta* **298**, 209–217
487 (1994).
- 488 36. Vance, D. & Thirlwall, M. An assessment of mass discrimination in MC-
489 ICPMS using Nd isotopes. *Chemical Geology* **185**, 227–240,
490 doi:10.1016/S0009-2541(01)00402-8 (2002).
- 491 37. Tanaka, T. et al. JNdi-1: a neodymium isotopic reference in consistency with
492 LaJolla neodymium. *Chemical Geology* **168**, 279–281, doi:10.1016/S0009-
493 2541(00)00198-4 (2000).
- 494 38. MacLeod, K. G., Martin, E. E. & Blair, S. W. Nd isotopic excursion across
495 Cretaceous ocean anoxic event 2 (Cenomanian-Turonian) in the tropical North
496 Atlantic. *Geology* **36**, 811–814, doi:10.1130/G24999a.1 (2008).
- 497 39. Piotrowski, A. M., Goldstein, S. L., Hemming, S. R. & Fairbanks, R. G.
498 Temporal relationships of carbon cycling and ocean circulation at glacial
499 boundaries. *Science* **307**, 1933–1938, doi:10.1126/Science.1104883 (2005).

- 500 40. R Core Team. R: A Language and Environment for Statistical Computing. *R*
501 *Foundation for Statistical Computing Vienna, Austria*, doi:[http://www.R-](http://www.R-project.org)
502 [project.org](http://www.R-project.org) (2014).
- 503 41. Goldstein, S. L. & Hemming, S. R. Long-lived isotopic tracers in
504 oceanography, paleoceanography, and ice-sheet dynamics. *Treatise on*
505 *geochemistry* **6**, 453–489 (2003).

506

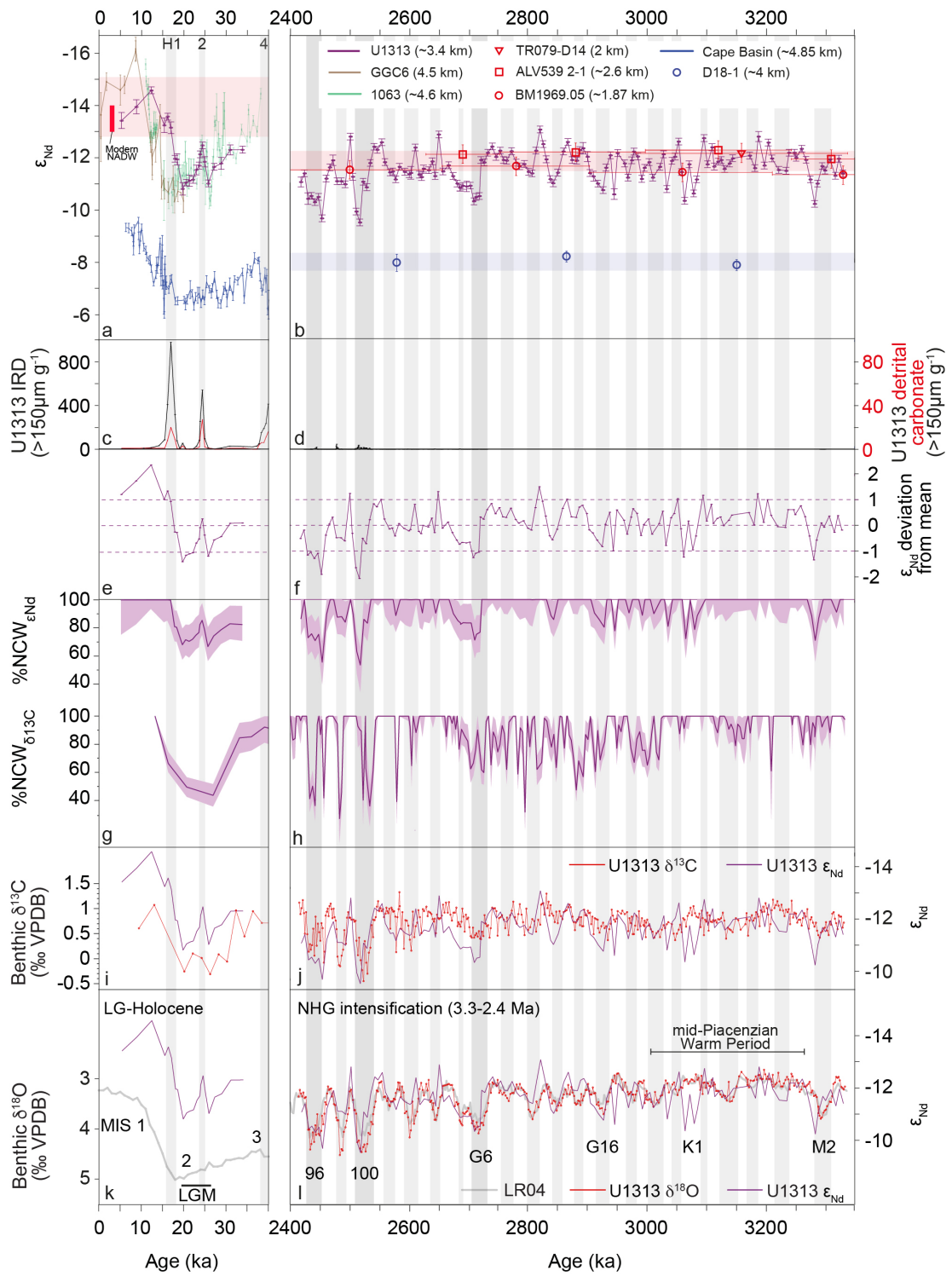


507

508

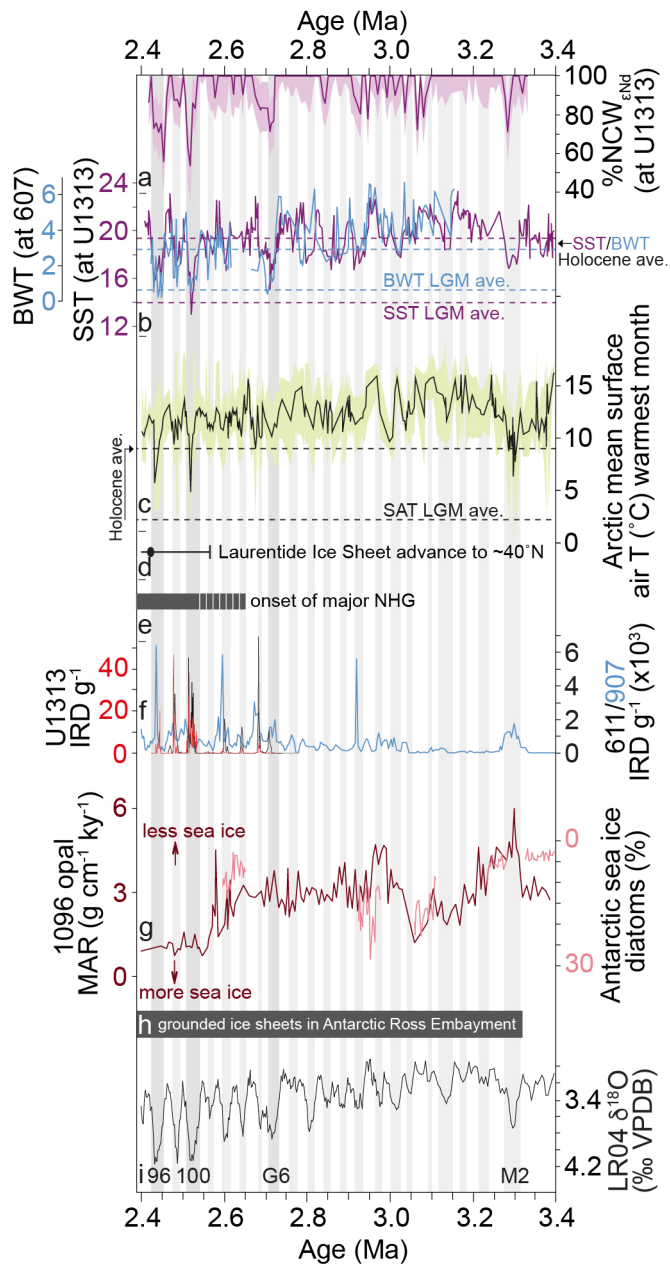
509

Figure 1.



510
511
512

Figure 2.



513
514
515
516

Figure 3.